# HYPERSPECTRAL DATA DECONVOLUTION FOR GALAXY KINEMATICS WITH MCMC

*Emma Villeneuve*[1,2], *Hervé Carfantan*[1,2]

(1) Université de Toulouse; UPS-OMP; IRAP; Toulouse, France
(2) CNRS; IRAP; 14, avenue Edouard Belin, F-31400 Toulouse, France

## ABSTRACT

The development of hyperspectral instruments requires new methods for data processing and analysis. We focus in this work on the estimation of the flux, position and width of spectral lines from astrophysical data, necessary to study the kinematics of galaxies. Classically used estimation methods, such as the method of moments and the maximum likelihood (ML), neglect the effect of the spatial Point Spread Function of the data acquisition system. The aim of this paper is to propose 3D deconvolution methods: the first is based on the ML estimator; a second introduces weak priors on the parameters and computes the posterior mean estimator with a Monte-Carlo Markov Chain, using a hybrid Gibbs/Metropolis-Hastings algorithm. The methods are compared on simulated hyperspectral data and the latter is shown to give the best results, in particular in the case of a low signal to noise ratio.

***Index Terms—***

Deconvolution, estimation, MCMC, hyperspectral data, Gibbs sampler, emission line, galaxy kinematics

## 1. INTRODUCTION

The development of hyperspectral instruments, able to perform at once the acquisition of images over a large number of wavelengths, is a revolution for scientists in remote sensing and astrophysics. Hyperspectral images not only correspond to the observation of an object in several wavelength bands, but associate to each pixel a full spectrum. Processing and analysis of such data present a challenge for the signal and image processing community. One example is MUSE [1], which will be a second generation instrument for one of the 8 meter diameter telescopes of the VLT at Paranal (Chile). MUSE aims at providing datacubes constituted of $300 \times 300$ pixel images (for a field of view of 1 arcmin$^2$ in the *Wide Field Mode*–WFM) with up to 4000 wavelengths in the visible spectrum, for each observation, with typical exposure times from a few minutes up to a few hours.

Our work is part of the DAHLIA project, which aims at developing new methods and algorithms adapted to the analysis and processing of such hyperspectral data. In particular, this project focuses on the fusion, deconvolution, source separation and source detection tasks. The main goal of this study is to present a reliable method to estimate the flux, the relative velocity and the velocity dispersion of a rotating galaxy, from hyperspectral data, which is necessary when studying the kinematics of a galaxy. As the hyperspectral data are blurred by the Point Spread Function (PSF) of the acquisition system, such estimations correspond to a 3D deconvolution problem.

In section 2, we briefly describe the different models for the data, Point Spread Function (PSF) and noise. Section 3 presents existing estimation methods, which work independently for each spatial position, not accounting for the spatial PSF. We introduce in section 4 a method based on the posterior mean estimator and stochastic sampling to solve this estimation problem. Then, we propose in section 5 a deconvolution method, generalizing the previous estimation method, estimating jointly the parameters for every spatial position, accounting for the spatial PSF. Finally some simulation results are shown in section 6.

## 2. PROBLEM STATEMENT

### 2.1. Model for the object

An emission line at a spatial position $\boldsymbol{s}$ can be simply modelled as a Dirac delta function $a(\boldsymbol{s})\delta(\lambda - \lambda_0)$ where $\lambda_0$ is the emission wavelength and $a(\boldsymbol{s})$ its corresponding flux. The expansion of the universe shifts the line in the spectral direction $\lambda$ (red-shift). Moreover, due to the galaxy's kinematics, the emission line is spectrally shifted and enlarged. As a first approximation, the resulting spectral line can be modelled with a Gaussian function:

$$\begin{aligned} \mathcal{L}(\boldsymbol{s},\lambda) &= \frac{a(\boldsymbol{s})}{\sqrt{2\pi}w(\boldsymbol{s})} \cdot \exp\left(-\frac{1}{2}\frac{(\lambda - c(\boldsymbol{s}))^2}{w(\boldsymbol{s})^2}\right) \\ &= a(\boldsymbol{s}) \cdot \boldsymbol{\ell}(c(\boldsymbol{s}), w(\boldsymbol{s}), \lambda) \end{aligned}$$

where $c(\boldsymbol{s})$ and $w(\boldsymbol{s})$ are the position and the width of the line. Studying the kinematics of a galaxy requires to estimate from the data the maps $a(\boldsymbol{s})$, $c(\boldsymbol{s})$ and $w(\boldsymbol{s})$ for each spatial position $\boldsymbol{s}$.

This work was partially supported by ANR project 08-BLAN-0253-01 DAHLIA - Dedicated Algorithms for HyperspectraL Imaging in Astronomy.

### 2.2. Point Spread Function (PSF) model

The observed object is blurred spatially and spectrally by the atmospheric effects, the telescope and the instrument. For MUSE data, the global 3D PSF can be considered separable in the spatial and spectral directions, denoted hereafter as FSF (Field SF) and LSF (Line SF) [2].

The FSF is mainly due to the effect of the atmosphere and the telescope on the data. In the WFM, without adaptive optics corrections, it is spatially invariant and slowly varying with respect to the wavelength. As we focus in this study on a small part of the datacube around an emission line, the FSF can be assumed spectrally invariant and is noted $F(\boldsymbol{s})$.

The LSF models the spectral spreading of MUSE instrument. It is slowly spectrally varying so it is approximately invariant for the considered part of the datacube. It is spatially varying and is noted $L_{\boldsymbol{s}}(\lambda)$.

Both the FSF and the LSF are supposed to be known: the first one, which depends on the seeing conditions, can be estimated from the data of an isolated star, while the second is deduced from the instrument's calibration stage.

### 2.3. Data model

The spectral line $\mathcal{L}(\boldsymbol{s},\lambda)$ is convolved by the LSF and FSF:

$$\mathcal{L}_{LF}(\boldsymbol{s},\lambda) = \iiint \mathcal{L}(\boldsymbol{s}',\lambda') \cdot L_{\boldsymbol{s}'}(\lambda'-\lambda) \cdot F(\boldsymbol{s}'-\boldsymbol{s}) d\lambda' d\boldsymbol{s}'$$

which will be noted hereafter $\mathcal{L}_{LF}(\boldsymbol{s},\lambda) = \mathcal{L}(\boldsymbol{\theta}) * \boldsymbol{L} * \boldsymbol{F}$ with $\boldsymbol{\theta}$ the parameters of the spectral line.

The noise-free data correspond to the addition of this convolved spectral line to the sky spectrum (which has been convolved by the LSF):

$$O(\boldsymbol{s},\lambda) = \mathcal{L}_{LF}(\boldsymbol{s},\lambda) + \text{sky}(\boldsymbol{s},\lambda).$$

Noise is mainly due to the photon counting process (readout noise being negligible) and is modelled as spatially and spectrally independent Poisson noise. However, due to a large integration time, it can be approximated as an additive Gaussian noise $n \sim \mathcal{N}(0,\Gamma(\boldsymbol{s},\lambda))$, with $\Gamma(\boldsymbol{s},\lambda) = O(\boldsymbol{s},\lambda)$. Finally, the sky spectrum is estimated and subtracted from the data:

$$D(\boldsymbol{s},\lambda) = \mathcal{L}_{LF}(\boldsymbol{s},\lambda) + n(\boldsymbol{s},\lambda).$$

Note that the noise variance $\Gamma(\boldsymbol{s},\lambda)$ may be very high, since the noise is partially due to the sky spectrum. It is unknown in practice but may be approximated by the data (before sky subtraction). An example of such data is illustrated Fig. 1, for 4 wavelengths around an emission line.

## 3. EXISTING ESTIMATION METHODS

We focus here on the classical methods used to estimate the characteristics of spectral lines, without taking into account the spatial convolution, which will be called hereafter "estimation methods". The aim is to estimate the parameters of the spectral lines $\boldsymbol{\theta}_k = [a_k, c_k, w_k]$ , for all spatial position $\boldsymbol{s}_k$ among $\{\boldsymbol{s}_1 \dots \boldsymbol{s}_N\}$. These classical methods do not account for the FSF, or equivalently approximate the FSF by a Dirac delta function $F(\boldsymbol{s}) = \delta(\boldsymbol{s})$, and therefore consider each spatial position $\boldsymbol{s}_k$ independently.

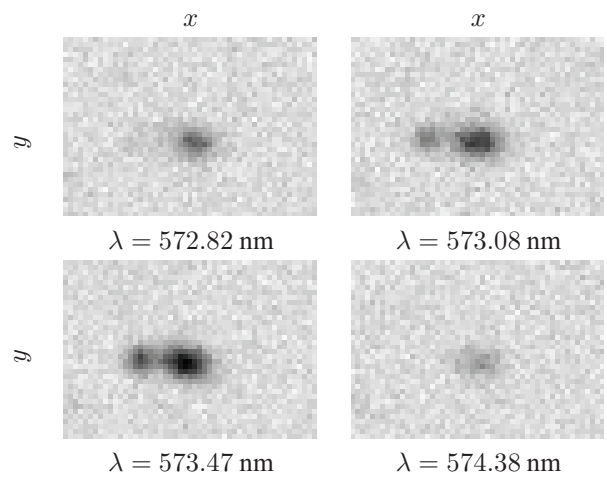


**Fig. 1**. Extracts of a simulated hyperspectral datacube at four different wavelengths. Contents: galaxy at the centre, other objects. Integration time: 80 hours. All pictures have the same inverse color scale.

### 3.1. Method of moments (MM)

The method of moments is commonly used by the astrophysical community to estimate spectral line characteristics [3]. First, the flux is estimated as the sum of the pixels' intensities along the spectral line. Then, the position and the width are estimated as the first and second order spectral moments of the data:

$$\text{Flux:} \quad \widehat{a_k} = \sum_i D(\boldsymbol{s}_k,\lambda_i)$$

$$\text{Position:} \quad \widehat{c_k} = \frac{1}{\widehat{a_k}} \sum_i \lambda_i D(\boldsymbol{s}_k,\lambda_i)$$

$$\text{Width:} \quad \widehat{w_k} = \sqrt{\frac{1}{\widehat{a_k}} \sum_i (\lambda_i - \widehat{c_k})^2 D(\boldsymbol{s}_k,\lambda_i)}.$$

For such a method, no assumption of the shape of the spectral line has to be done. As the LSF is not taken into account explicitly, the estimated quantities do not correspond exactly to the characteristics of the spectral line $\mathcal{L}(\boldsymbol{s}_k,\lambda)$, even for an ideal FSF (Dirac). Nevertheless, in this ideal case, if the LSF is symmetric, the position of the line is not affected by the spectral convolution, so $\widehat{c_k}$ gives a non-biased estimator of $c_k$. Furthermore, if both the LSF and the emission line are assumed to have a Gaussian shape, the line can be spectrally deconvolved by subtracting to the square of the estimated width $\widehat{w}_k$ the variance of the LSF. The main drawback of such a method is that it is generally very sensitive to the noise (note that the noise characteristics are not accounted for), in particular for the width estimation.

### 3.2. Maximum likelihood estimator (ML)

For the noise model of § 2.3, data $\boldsymbol{d}_k = \{D(\boldsymbol{s}_k, \lambda_i)\}_i$ have a Gaussian distribution. If we note $\mathcal{L}(\boldsymbol{\theta}_k) * L_k$ the spectral convolution of the line of parameters $\boldsymbol{\theta}_k$ with the LSF at spatial position $\boldsymbol{s}_k$, the likelihood can be written:

$$p(\boldsymbol{d}_k|\boldsymbol{\theta}_k) \propto \mathcal{G}\left(\boldsymbol{d}_k - \mathcal{L}(\boldsymbol{\theta}_k) * L_k, \boldsymbol{\Gamma}_k\right)$$

where $\mathcal{G}(\boldsymbol{u}, \boldsymbol{\Gamma}) = \exp\left(-\frac{1}{2}\|\boldsymbol{u}\|^2_{\boldsymbol{\Gamma}^{-1}}\right)$, $\|\boldsymbol{u}\|^2_{\boldsymbol{\Gamma}^{-1}} = \boldsymbol{u}^T\boldsymbol{\Gamma}^{-1}\boldsymbol{u}$, and $\boldsymbol{\Gamma}_k = \text{diag}\{\Gamma(\boldsymbol{s}_k, \lambda_i)\}_i$. So, the maximum likelihood estimator of $\boldsymbol{\theta}_k$ is defined as:

$$\widehat{\boldsymbol{\theta}}_{\text{ML},k} = \arg\min_{\boldsymbol{\theta}_k} \|\boldsymbol{d}_k - \mathcal{L}(\boldsymbol{\theta}_k) * L_k\|^2_{\boldsymbol{\Gamma}_k^{-1}}$$

The criterion to be minimized is not convex and may have local minima. So, depending on the algorithm used to compute the estimate, it can be very sensitive to the initialisation.

## 4. PROPOSED ESTIMATION METHODS

To improve the spectral line parameters estimation, we propose to use Monte-Carlo estimation methods, which are efficient alternatives to optimisation methods, especially when the criterion has local minima. Indeed, such methods give estimates which are theoretically independent from the initialisation. Moreover, such a strategy also gives essential information in terms of confidence levels (more precisely variances) associated to the estimated parameters.

The posterior distribution of the parameters $p(\boldsymbol{\theta}_k|\boldsymbol{d}_k)$ can be derived from the likelihood, through Bayes' rule $p(\boldsymbol{\theta}_k|\boldsymbol{d}_k) = p(\boldsymbol{d}_k|\boldsymbol{\theta}_k)p(\boldsymbol{\theta}_k)$, introducing prior distribution $p(\boldsymbol{\theta}_k)$ on the parameters. Then, random vectors $\boldsymbol{\theta}_k$ are generated, building a Markov chain $\{\boldsymbol{\theta}_k^{(i)}\}_{i=1\ldots P}$, whose stationary distribution is the posterior distribution $p(\boldsymbol{\theta}_k|\boldsymbol{D}_k)$. For this purpose, we use a hybrid Gibbs/Metropolis-Hastings algorithm, which generates random values according to the conditional distribution of the parameters. Finally, the Posterior Mean (PM) estimator is computed from these samples, as well as its variance. Each of the ingredients of the proposed method are described hereafter.

### 4.1. Prior distributions

We have chosen to introduce weak prior information on the parameters, so as not to introduce bias in the estimation. The parameters are considered independent $p(\boldsymbol{\theta}_k) = p(a_k)p(c_k)p(w_k)$, where:

• $a_k$ is positive Gaussian of variance $r_a$: $\sim \mathcal{N}^+(0; r_a)$ with a spatially constant large value $r_a$:
$p(a_k) = 2\frac{1}{\sqrt{2\pi r_a}} \exp\left(-\frac{1}{2}\frac{a_k^2}{r_a}\right) \mathbb{1}_{[0;+\infty[}(a_k)$.

• $c_k$ is uniformly distributed on an interval $[\lambda_1; \lambda_2]$ determined from the data: $p(c_k) = \frac{1}{\lambda_2 - \lambda_1}\mathbb{1}_{[\lambda_1;\lambda_2]}(c_k)$.

• $w_k$ is uniformly distributed on the interval $[0; \omega]$ with $\omega$ the maximal width of the line, which can be evaluated from the data: $p(w_k) = \frac{1}{\omega}\mathbb{1}_{[0;\omega]}(w_k)$.

### 4.2. Conditional distributions

The conditional posterior distributions of the parameters are deduced from the prior distributions and the likelihood:

• $p(a_k|c_k, w_k, \boldsymbol{d}_k) \propto \mathcal{G}\left(a_k - \mu, \rho\right) \mathbb{1}_{[0;+\infty[}(a_k)$,
where $\mu = \rho\, \boldsymbol{f}_k^T\boldsymbol{\Gamma}_k^{-1}\boldsymbol{d}_k$ and $\rho = \dfrac{r_a}{1 + r_a \boldsymbol{f}_k^T\boldsymbol{\Gamma}_k^{-1}\boldsymbol{f}_k}$,
with $\boldsymbol{f}_k = \boldsymbol{\ell}(c_k, w_k, \lambda) * L_k(\lambda)$.

• $p(c_k|a_k, w_k, \boldsymbol{d}_k) \propto \mathcal{G}\left(\boldsymbol{d}_k - \mathcal{L}(\boldsymbol{\theta}_k) * L_k, \boldsymbol{\Gamma}_k\right) \mathbb{1}_{[\lambda_1;\lambda_2]}(c_k)$.

• $p(w_k|a_k, c_k, \boldsymbol{d}_k) \propto \mathcal{G}\left(\boldsymbol{d}_k - \mathcal{L}(\boldsymbol{\theta}_k) * L_k, \boldsymbol{\Gamma}_k\right) \mathbb{1}_{[0;\omega]}(w_k)$.

### 4.3. Hybrid Gibbs/Metropolis-Hastings algorithm

Instead of generating directly random vectors from the joint posterior distribution $p(\boldsymbol{\theta}_k|\boldsymbol{d}_k)$, we propose to use a Gibbs sampler. Such an algorithm generates random variables from the conditional posterior distributions given above, for each individual parameter of $\boldsymbol{\theta}_k$. Generalizing such an algorithm for the deconvolution problem will be straightforward.

If the flux parameter can be generated directly from a truncated Gaussian distribution [4], the densities for the position and width parameters are not easy to sample directly. Therefore we use a Metropolis-Hastings step with a Gaussian proposal distribution, the variance of which is adjusted to obtain an optimal acceptance rate [5]. Estimated parameters $\widehat{\boldsymbol{\theta}}_{\text{PM},k}$ and corresponding variances are computed from the samples, the process being performed independently for each $\boldsymbol{s}_k$.

## 5. DECONVOLUTION METHODS

The main drawback of previous methods is that they do not take into account the spatial spreading due to the FSF. Thus the estimated parameters do not correspond to the parameter of the emission lines (see § 6.2). Therefore we propose to perform a true 3D deconvolution, estimating jointly the spectral lines parameters $\boldsymbol{\theta} = \{\boldsymbol{\theta}_k\}_k$ for every spatial position, accounting for the 3D PSF (FSF and LSF).

The proposed deconvolution method is a generalisation of the estimation method proposed in § 4:

• As the noise is spatially independent, the likelihood corresponds to the product of the likelihoods for each spatial position and can be noted:

$$p(\boldsymbol{D}|\boldsymbol{\theta}) \propto \mathcal{G}\left(\boldsymbol{D} - \mathcal{L}(\boldsymbol{\theta}) * \boldsymbol{L} * \boldsymbol{F}, \boldsymbol{\Gamma}\right),$$

where $\boldsymbol{D}$ and $\boldsymbol{\Gamma}$ collect all the data and their corresponding variance. Therefore, the joint maximum likelihood (JML) estimator of parameters $\boldsymbol{\theta}$ corresponds to:

$$\widehat{\boldsymbol{\theta}}_{\text{JML}} = \arg\min_{\boldsymbol{\theta}} \|\boldsymbol{D} - \mathcal{L}(\boldsymbol{\theta}) * \boldsymbol{L} * \boldsymbol{F}\|^2_{\boldsymbol{\Gamma}^{-1}}.$$

• The parameters for each spatial position are considered *a priori* independent: $p(\boldsymbol{\theta}) = \prod_k p(\boldsymbol{\theta}_k)$.

• Let $\boldsymbol{U}_k = \boldsymbol{D} - \sum_{j \neq k} a_j \boldsymbol{f}_j \delta(\boldsymbol{s}_j) * \boldsymbol{F}$ be the residual of the contribution of the spectral lines for each spatial position excepted position $\boldsymbol{s}_k$. Then, the conditional posterior distributions have an expression very similar to the estimation case:

– $p(c_k|\boldsymbol{\theta}_{\text{rest}}, \boldsymbol{D}) \propto \mathcal{G}\left(\boldsymbol{U}_k - \mathcal{L}(\boldsymbol{\theta}_k) * L_k * \boldsymbol{F}, \boldsymbol{\Gamma}\right) \mathbb{1}_{[\lambda_1;\lambda_2]}(c_k)$

– $p(w_k|\boldsymbol{\theta}_{\text{rest}}, \boldsymbol{D}) \propto \mathcal{G}\left(\boldsymbol{U}_k - \mathcal{L}(\boldsymbol{\theta}_k) * L_k * \boldsymbol{F}, \boldsymbol{\Gamma}\right) \mathbb{1}_{[0;\omega]}(w_k)$

– $p(a_k|\boldsymbol{\theta}_{\text{rest}}, \boldsymbol{D}) \propto \mathcal{G}\left(a_k - \mu, \rho\right) \mathbb{1}_{[0;+\infty[}(a_k)$

where $\mu = \rho\, \boldsymbol{e}_k^T \boldsymbol{\Gamma}^{-1} \boldsymbol{U}_k$ and $\rho = \dfrac{r_a}{1 + r_a \boldsymbol{e}_k^T \boldsymbol{\Gamma}^{-1} \boldsymbol{e}_k}$, with $\boldsymbol{e}_k = \boldsymbol{f}_k \delta(\boldsymbol{s}_k) * \boldsymbol{F}$.

• As for the proposed estimation method, these conditional distributions can be used to generate samples from the joint posterior distribution $p(\boldsymbol{\theta}|\boldsymbol{D})$ using a hybrid Gibbs/Metropolis-Hastings algorithm. The joint posterior mean (JPM) estimated parameters $\widehat{\boldsymbol{\theta}}_{\text{JPM}}$ and their corresponding variances are computed from these samples.

## 6. SIMULATION RESULTS

### 6.1. Simulations

We have simulated data according to the models[1] of § 2 for Gaussian FSF and LSF, sampled at MUSE datacube resolution ($\Delta s = 0.2$ asec and $\Delta\lambda = 0.13$ nm). Note that for sake of simplicity, we have used 2D simulations, with one spatial and one spectral dimension instead of 3D (two spatial dimensions). Typical flux, position and width maps were used for these simulations, displayed Fig. 3 and 4 (with a thick red line)[2]. The FSF corresponds to bad seeing conditions, to emphasize the interest in deconvolution methods. Data were simulated with two noise levels; the first one, corresponding to a high SNR, usefull to validate the estimation and deconvolution methods. The second one, with a low SNR, corresponds to more realistic data. The resulting data are illustrated Fig. 2.

We used the mean squared errors (MSEs) to quantify the estimation error. The MM and ML estimates are thresholded before computing the MSEs, to have a value in the range used as prior for the PM estimator ($\lambda_1 = 5$, $\lambda_2 = 15$ for $c$ and $\omega = 2.5$ for $w$). MSEs on $c$ and $w$ are computed only for spatial positions from 8 to 22 as 99.6% of the flux of the galaxy lies between these positions.

[1] In fact, the simulated spectral line corresponds to the O-II spectral doublet. But, as both lines are assumed to have same flux and width, and the distance between them is known, the characteristics of the estimation and deconvolution problems are not fundamentally modified.

[2] The authors would like to thanks R. Bacon and the MUSE Consortium for providing the realistic MUSE simulations used to build the data.

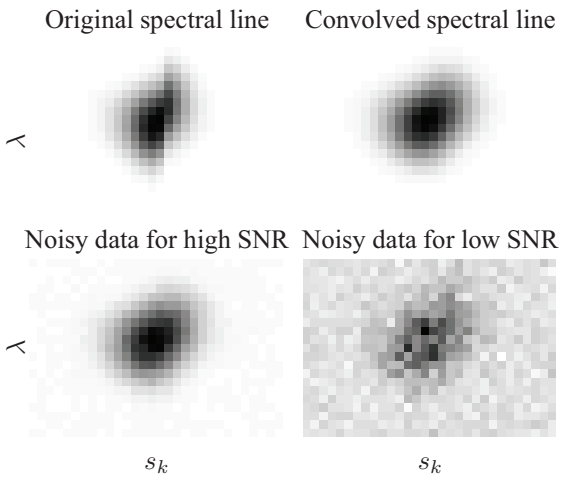


**Fig. 2**. 2D simulated data : $21 \times 30$ pixels in spectral (vertical) and spatial (horizontal) dimensions.

### 6.2. Estimation results

The ML estimates were computed with the Matlab function *fminsearch*, initialized with the results of the MM. PM estimates and it associated variances are computed from $P = 50\,000$ samples of the Markov Chain, after discarding the first $P$ samples of the chain.

In the case of a high SNR, the MM, ML and PM estimators give very similar results as shown for the estimated parameters on Fig. 3 and on the MSEs on Tab. 1. The estimated parameters clearly don't match with the theoretical values: in particular the flux and the position appear more spread and the width larger than the original ones, which was expected as the FSF hasn't been taken into account. In the more realistic case of low SNR, the results of the MM and ML are significantly worsened, which is not the case for the PM.

| | High SNR case | | | Low SNR case | | |
|---|---|---|---|---|---|---|
| | MM | ML | PM | MM | ML | PM |
| $\widehat{\boldsymbol{a}}$ | 2.46 | 2.47 | 2.49 | 3.48 | 3.53 | 3.79 |
| $\widehat{\boldsymbol{c}}$ | 0.26 | 0.22 | 0.22 | 0.77 | 0.51 | 0.44 |
| $\widehat{\boldsymbol{w}}$ | 0.14 | 0.11 | 0.11 | 0.84 | 0.32 | 0.087 |

**Table 1**. MSE for the estimation results.

### 6.3. Deconvolution results

As the optimisation algorithm used to compute JML (Matlab function *fminsearch*) may be sensitive to the initialisation, we used two initial values: the results of the ML estimation method and the true parameters. The corresponding results are denoted respectively JML and JML$^+$ hereafter.

Fig. 4 and Tab. 2 illustrate the deconvolution results obtained by the JML, JML$^+$ and JPM estimators, both in the high and low SNR cases. If the improvement of the deconvo-

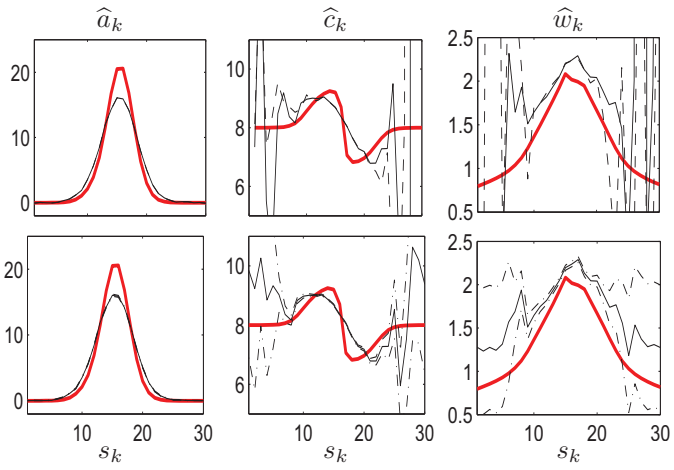


**Fig. 3**. **Estimation results:** theoretical (red thick line) and estimated flux, position and width for spatial position $s_k$. First row: MM (- -) and ML (–) estimates. Second row: PM (–) estimates +/- posterior standard deviation (–·).

lution methods is obvious on the estimated flux, it is not the case for the position and width estimated with JML, even in the high SNR case. This is due to the alternating high and low values of the estimated position $\widehat{c}_k$ for neighbouring spatial positions $s_k$, which effects cancel out after convolution with the FSF. Note that a different initialisation gives another result, but even with an ideal initialisation, the results of JML$^+$ are subject to the same alternating phenomenon. The results of JPM are better than the JML ones, in particular in the low SNR case. Both the flux and positions are well estimated, the latter being overestimated for the spatial positions with a very low flux, which is not physically significant. However, the width is not correctly retrieved with the JPM in the low SNR case.

| | High SNR case | | | Low SNR case | | |
|---|---|---|---|---|---|---|
| | JML | JML$^+$ | JPM | JML | JML$^+$ | JPM |
| $\widehat{a}$ | 1.93 | 0.38 | 0.18 | 7.92 | 5.32 | 2.15 |
| $\widehat{c}$ | 1.35 | 0.89 | 0.14 | 2.15 | 2.20 | 0.28 |
| $\widehat{w}$ | 0.33 | 0.40 | 0.052 | 0.90 | 1.48 | 0.18 |

**Table 2**. MSE for the deconvolution results.

As a conclusion, the proposed joint posterior mean deconvolution method improves the results of the classical estimation methods, which do not account for the spatial PSF. Moreover, it gives better results than the joint maximum likelihood estimates, even if the latter is initialized with the true parameters values.

## 7. REFERENCES


[1] R. Bacon, M. Accardo, and L. Adjali *et al.*, "The MUSE second-generation VLT instrument," *SPIE Conference Series*, vol. 7735, July 2010.

[2] E. Villeneuve, H. Carfantan, A. Jarno, D. Serre, V. Mazet, and S. Bourguignon, "Modélisation et estimation de la PSF d'un instrument hyperspectral au sol pour l'astrophysique," *Gretsi*, September 2011.

[3] B. Epinat, *Des galaxies proches aux galaxies lointaines : Étude cinématique et dynamique*, Ph.D. thesis, Université de Provence, November 2008.

[4] V. Mazet, D. Brie, and J. Idier, "Simulation of Positive Normal Variables using several Proposal Distributions," *IEEE Worshop Statistical Signal Processing*, July 2005.

[5] G. O. Roberts and J. S. Rosenthal, "Optimal scaling for various Metropolis-Hastings algorithms," *Statistical Science*, vol. 16, no. 4, pp. 351–367, 2001.


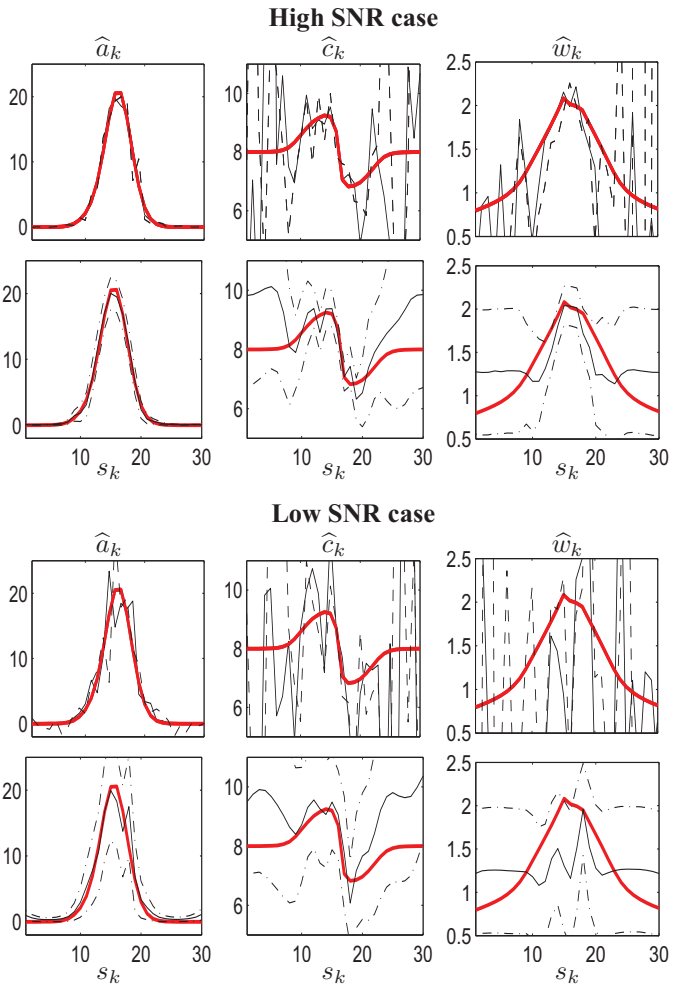


**Fig. 4**. **Deconvolution results for the high and low SNR cases:** theoretical (red thick line) and estimated flux, position and width for spatial position $s_k$. First rows: JML (- -) and JML$^+$ (–) estimates. Second rows: JPM (–) estimates +/- posterior standard deviation (–·).